ACS APPLIED MATERIALS & INTERFACES

Research Article

www.acsami.org

Insight into Sulfur Reactions in Li–S Batteries

Rui Xu,[†,⊥] Ilias Belharouak,*[,†,‡] Xiaofeng Zhang,[†] Rita Chamoun,[‡] Cun Yu,[§] Yang Ren,[§] Anmin Nie,[∥] Reza Shahbazian-Yassar,[∥] Jun Lu,[†] James C.M. Li,[⊥] and Khalil Amine[†]

[†]Chemical Sciences and Engineering Division, Argonne National Laboratory, 9700 South Cass Avenue, Argonne, Illinois 60439, United States

[‡]Qatar Environment and Energy Research Institute, Qatar Foundation, P.O. Box 5825, Doha, Qatar

[§]Advanced Photon Source, Argonne National Laboratory, 9700 South Cass Avenue, Argonne, Illinois 60439, United States

[∥]Department of Mechanical Engineering–Engineering Mechanics, Michigan Technology University, Houghton, Michigan 49931, United States

[⊥]Materials Science Program, Department of Mechanical Engineering, University of Rochester, Rochester, New York 14627, United States

Supporting Information

ABSTRACT: Understanding and controlling the sulfur reduction species (Li_2S_x, $1 \le x \le 8$) under realistic battery conditions are essential for the development of advanced practical Li–S cells that can reach their full theoretical capacity. However, it has been a great challenge to probe the sulfur reduction intermediates and products because of the lack of methods. This work employed various ex situ and in situ methods to study the mechanism of the Li–S redox reactions and the properties of Li_2S_x and Li_2S. Synchrotron high-energy X-ray diffraction analysis used to characterize dry powder deposits from lithium polysulfide solution suggests that the new crystallite phase may be lithium polysulfides. The formation of Li_2S crystallites with a polyhedral structure was observed in cells with both the conventional (LiTFSI) electrolyte and polysulfide-based electrolyte. In addition, an in situ transmission electron microscopy experiment observed that the lithium diffusion to sulfur during discharge preferentially occurred at the sulfur surface and formed a solid Li_2S crust. This may be the reason for the capacity fade in Li–S cells (as also suggested by EIS experiment in Supporting Information). The results can be a guide for future studies and control of the sulfur species and meanwhile a baseline for approaching the theoretical capacity of the Li–S battery.

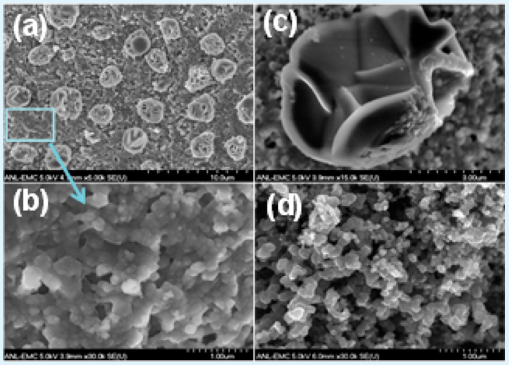

KEYWORDS: *lithium–sulfur (Li–S) batteries, sulfur chemistry, Coulombic efficiency, lithium polysulfide, EIS study*

1. INTRODUCTION

The rechargeable Li–S battery is based on the reversible redox process between sulfur and lithium [$S_8 + 16Li^+ + 16e^- \leftrightarrow 8Li_2S$]. Consequently, the sulfur cathode offers a superior theoretical capacity (1672 mAh g^{-1}) compared to conventional Li-ion battery cathodes.[1−8] Typically, Li–S cells in current research use elemental sulfur as the cathode, an organic liquid with lithium bis(trifluoromethanesulfonyl)-imide (LiTFSI) dissolved in a mixture of 1,3-dioxolane (DOL) and 1,2-dimethoxyethane ether (DME) solvents (1:1 ratio by volume) as the electrolyte, and lithium metal as the anode.

Researchers from academia and industry alike consider Li–S batteries promising and have dedicated considerable effort to developing the system. One of the great practical challenges in accessing the full theoretical capacity of sulfur is to solve the problems of low Coulombic efficiency and rapid capacity fading that are inherent to Li–S cells. These two problems are closely related to the formation of the intermediate sulfur discharge species, lithium polysulfides (Li_2S_x) (x = 3–8), and also final discharge product, Li_2S. Having a very low electronic and ionic conductivity, the Li_2S that is formed during discharge on the surface of the cathode may create an insulation barrier that prevents the full reduction of sulfur. Lithium polysulfides, on the other hand, have a complex chemistry and exist in different species in organic solvents. The dissolution of Li_2S_x from the S cathode to electrolyte and its subsequent migration to the anode causes shuttle reactions, a serious issue that leads to the loss of active cathode materials and corrosion of the lithium anode. Meanwhile, significant changes of the cathode morphology can result from polysulfide dissolution and possibly destroy the delicately designed structures of the sulfur electrode. As the practical performance of the Li–S battery is greatly impacted by the chemistry of sulfur reduced species, understanding and controlling their complex chemistry is

Received: May 30, 2014
Accepted: November 26, 2014
Published: November 26, 2014

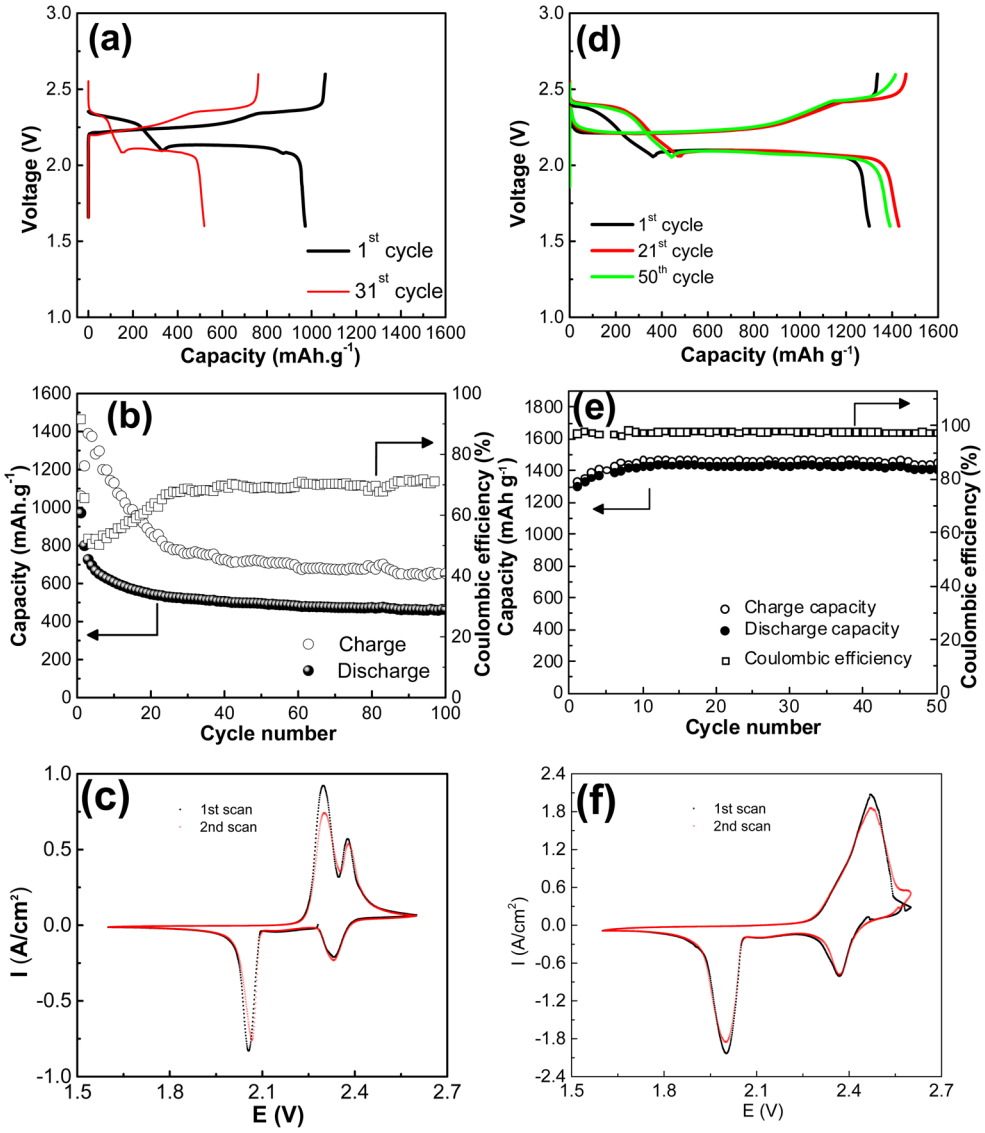

Figure 1. Performance of Li–S cell containing 1 M LiTFSI in DME/DOL (v/v = 1/1) electrolyte: (a) charge–discharge voltage profiles, (b) capacity and Coulombic efficiency vs cycle number at C/10, and (c) CV curves. Performance of Li–S cell containing polysulfide electrolyte: (d) charge–discharge voltage profiles, (e) capacity and Coulombic efficiency vs cycle number at C/10, and (f) CV curves.

essential to approaching the full theoretical capacity of Li–S cells.

To solve the issues related to the formation, dissolution, and migration of lithium polysulfides in Li–S cells, researchers have pursued different approaches.[9−32] Great efforts have been devoted to confining sulfur in carbons, aiming to prevent the dissolution of lithium polysulfides.[9−26] It was also tried to protect the anode by either adopting electrolyte additives, using new solvents or passivating the lithium metal surface.[27−32] In our previous work, it was found that adopting a polysulfide-based electrolyte could mitigate the dissolution of Li_2S_x from the cathode to the electrolyte.[33] Meanwhile, this electrolyte also paves the way for using Li_2S cells by eliminating the potential barrier in the initial charge of Li_2S when using the LiTFSI electrolyte.[34] However, the mechanism of the sulfur reduction chemistry is not clear yet owing to the difficulty in characterizing the intermediate species Li_2S_x and the final product Li_2S during the electrochemical reactions, as these species were considered to be poorly crystallized and, therefore, do not provide much information when subjected to conventional X-ray analysis techniques.

Understanding the Li_2S_x electrochemistry and chemistry can facilitate the control of the sulfur species in practical Li–S batteries. In this work, we focused on probing the mechanism of the Li–S redox reactions and the chemistry of Li_2S_x and Li_2S. Synchrotron high-energy X-ray diffraction analysis was used to characterize synthesized dry lithium polysulfide powder that was found to be crystalline. There have been several excellent studies investigating the properties of lithium polysulfide solutions,[26,27,35−46] but the study of solid lithium polysulfide is scarce. We also analyzed the morphological and structural changes of the sulfur electrode at different depths of discharge, and Li_2S crystallites with polyhedral architecture were observed in both the conventional LiTFSI electrolyte and the polysulfide-based electrolyte. In addition, an in situ transmission electron microscopy (TEM) experiment detected Li_2S covering the sulfur surface during discharge. This technique enables the observation of the Li–S redox process in a similar environment to a real Li–S cell. In the Supporting Information, electro-

chemical impedance spectra (EIS) of Li−S half cells were obtained to study the electrochemical behavior at the electrode/electrolyte interfaces. The EIS results showed that the formation of Li_2S led to a large increase of resistance in the medium to low frequency range in the cell.

2. EXPERIMENTAL SECTION

Lithium disulfide, sulfur, and lithium nitrate powders, as well as dimethoxyethane (DME) solvent, were purchased from Sigma-Aldrich. Lithium polysulfide (Li_2S_x, x = 4−9) solutions and powders were prepared by weighing an appropriate amount of Li_2S and S and stirring them together in DME at 50 °C until no precipitates were left. The ratios of Li_2S and S added to the solution were 1:3, 1:5, 1:7, and 1:8. Even though the resulting solution contains lithium polysulfides with various molecular entities, we are using the designations Li_2S_4, Li_2S_6, Li_2S_8, and Li_2S_9 to represent the different ratios of Li_2S and S added initially to the solvent. Thus, this terminology does not necessarily mean that the solution contains only one chemical species. All experimental works were done inside an argon-filled glovebox with oxygen and water levels less than 1 ppm.

Dry powder deposits were prepared by slowly drying the polysulfide solutions in an argon-filled glovebox at room temperature. This process usually takes a few weeks because when the solution becomes highly viscous after the solvent evaporates, it takes time for the sample to dry completely.

The polysulfide electrolyte was prepared by mixing stoichiometric Li_2S and S (molar ratio Li_2S:S = 1:8) and stirring them together in DME at 50 °C. Subsequently, $LiNO_3$ was added to the solution until it dissolved completely, forming a dark red polysulfide electrolyte solution (0.2 M Li_2S_9 and 0.5 M $LiNO_3$ in DME).

Electrochemical performance was evaluated in tests with CR2032-type coin cells (1.6 cm^2). A slurry of sulfur powder (60 wt %), acetylene carbon (30 wt %), and pol(vinylidene fluoride) binder (10 wt %) was mixed in a mortar by hand and coated onto an aluminum foil. An electrode was prepared in a glovebox filled with argon atmosphere, and was dried at 60 °C in a vacuum oven overnight. The loading of sulfur in the electrode was around 0.8 mg cm^{-2}. Two electrolytes were prepared: (1) 1 M LiTFSI dissolved in a mixture of DOL and DME solvents (1:1 ratio by volume) and (2) a polysulfide electrolyte consisting of 0.2 M Li_2S_9 and 0.5 M $LiNO_3$ dissolved in DME. The cells were assembled with lithium metal as the anode. The amount of electrolyte used in each cell was 0.02 mL. The Li_2S_9 content in the polysulfide electrolyte contained in each cell was around 1.2 mg. The coin cells were tested in the galvanostatic mode at room temperature within a voltage range 1.6−2.6 V using a Maccor multichannel battery cycler. The current density for charge and discharge was 160 mA g^{-1} (corresponding to a charge/discharge rate of roughly 0.1 C).

Synchrotron X-ray (115 keV, λ = 0.108 Å) powder diffractions were obtained at beamline 11-ID-C at the Advanced Photon Source of Argonne National Laboratory. Fit2D software was applied to convert the 2-D diffraction patterns to 1-D diffraction patterns. The obtained XRD patterns were converted to those corresponding to the Cu Kα wavelength (λ = 1.54 Å). The morphologies of the electrodes were investigated by scanning electron microscopy (SEM) using a Hitachi S-4700-II microscope in the Electron Microscopy Center of Argonne National Laboratory. An in situ microscopic characterization was performed on JEOL 3010−300 keV high-resolution transmission electron microscopy (HR-TEM) with a single-tilt STM holder (Nanofactory). A constant voltage bias (−3.0 V) was applied to the cell in the in situ TEM experiment. A constant voltage bias was applied to the terminal during the in situ analysis. The electrochemical impedance spectroscopy (EIS) of the cells was measured on a Solartron analytical 1470E cell test system coupled with 1400 FRA impedance analyzer.

3. RESULTS AND DISCUSSION

The performance of a Li−S cell is greatly determined by the chemistry of the sulfur species. In a typical Li−S cell, the conventional electrolyte (LiTFSI in DME-DOL) and a sulfur electrode prepared by simply mixing the sulfur and acetylene black powders were adopted. The cell shows high initial capacity but quick capacity fade over cycling and low Coulombic efficiency because of the dissolution of lithium polysulfide species, shuttle reactions, and other contributing factors, such as the formation of an insulating Li_2S layer. Figure 1a shows the voltage profiles of the cell, which consist of two plateaus in the discharge and charge, in agreement with previous results.[1,3,39] In a typical Li−S cell, lithium polysulfides (Li_2S_x, where x = 4−8) with long chains are generated at a high voltage plateau (2.3−2.4 V), and further reduction of these polysulfides to Li_2S_2 and/or Li_2S occurs at a lower voltage plateau (∼2.1 V). We observed more capacity in the charge than in the discharge starting from the second cycle, indicating the occurrence of a shuttle reaction (Figure 1a). After 50 cycles, the cell capacity had faded dramatically, from about 1000 to 560 mAh/g for discharge and 1500 to 650 mAh/g for charge, which translates to a Coulombic efficiency of approximately 70% (Figure 1b). Such capacity fade and low Coulombic efficiency are common features for Li−S electrodes that do not confine sulfur within porous carbon or use modified electrolytes, as the dissolution of lithium polysulfide intermediates into the electrolyte promotes active sulfur loss and shuttle reactions.[3,8,38,39] Cyclic voltammetry (CV) testing was also performed on a cell with the same configuration at a scan rate of 0.028 mV/s. As shown in Figure 1c, the cell displays two cathodic peaks (at 2.06 and 2.35 V) and two anodic peaks (at 2.28 and 2.39 V). The results match well the charge and discharge voltage profiles of the cell.

The performance of Li−S cells can be greatly improved by controlling the chemical equilibria of the lithium polysulfide species in Li−S cells. While much effort has been devoted to confining sulfur in the electrode,[9−18] we aimed to mitigate the dissolution of Li_2S_x and shuttle reactions by leveling the concentration gradient of the polysulfide species at the cathode/electrolyte interface. We employed a polysulfide-based electrolyte (0.2 M Li_2S_9 and 0.5 M $LiNO_3$ dissolved in DME) as an alternative to the conventional LiTFSI electrolyte. A similar sulfur electrode as in the previous cell was prepared by simply mixing acetylene black and sulfur powders. As shown in Figure 1d,e, a stable discharge capacity of 1450 mAh/g (calculated on the basis of the sulfur content in the cathode) was delivered by the cell using this electrolyte.[33] No obvious capacity fade occurred during the first 50 cycles, and the Coulombic efficiency was about 98%, as shown in Figure 1e. The CV curves (Figure 1f), compared to the curves of the cell using the LiTFSI electrolyte, indicated a larger polarization due to the lower conductivity of the polysulfide-based electrolyte (Supporting Information Figure S5).[33] Although the polysulfide-based electrolyte has a lower ionic conductivity, the cell still has a superior performance over that with the LiTFSI electrolyte. We believe that the predissolved polysulfide speices in the electrolyte should have assisted in balancing the concentration gradient of the polysulfides at the sulfur/electrolyte interface, the consequence of which would be decreased polysulfide dissolution and increased sulfur utilization. This demonstrates that controlling the chemical equilibria

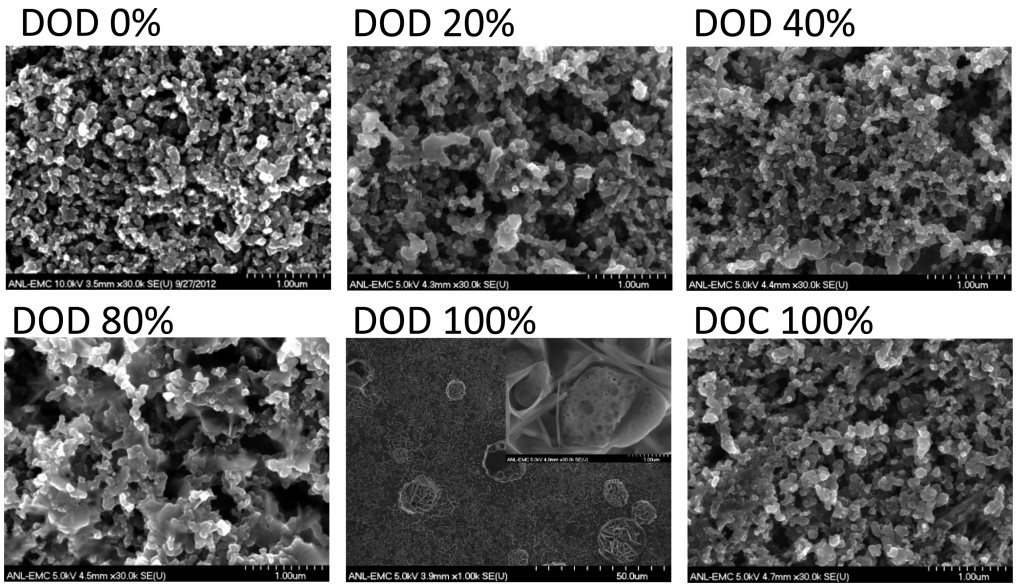

Figure 2. Surface morphology of sulfur electrode at different depths of discharge and charge, tested using the LiTFSI electrolyte.

of sulfur species can greatly influence the Coulombic efficiency, cycling stability, and charge−discharge capacity of Li−S cells.

It should be noted that the polysulfide electrolyte also contributes to the overall battery capacity. As shown in our previous work,[33] the polysulfide electrolyte itself demonstrated an increasing capacity that stabilized at around 350 mAh g^{-1} after 15 cycles. This small value suggests that a significant amount of lithium polysulfides remained in the electrolyte being electrochemically inactive and ionic conductive. This feature enables the use of lithium polysulfides as an electrolyte salt.

To study the morphologies of the sulfur electrodes at different stages of the electrochemical process during which Li_2S_x was produced, sulfur electrodes were salvaged from cells at different depths of discharge (DOD) during the first cycle with the presence of LiTFSI electrolyte and studied by SEM (Figure 2). The pristine sulfur electrode (0% DOD) was uniform, indicating a good mixing of sulfur and carbon. At the early stages of discharge (DOD = 20% and 40%), the voids and large porosities indicated that sulfur was partially converted to lithium polysulfides in the electrolyte. When preparing the sulfur electrodes, we choose not to encapsulate sulfur into porous carbons in order to observe the morphology change during charge/discharge because of the dissolution and redeposition of lithium polysulfide and also the recrystallization of the Li_2S. The morphological changes of the sulfur electrodes during the discharge process suggest that the sulfur electrode lost a large amount of its active material during reduction. At 80% DOD, the sulfur electrode became highly porous, and an obvious swelling of the electrode was seen. Interestingly, crystallite with polyhedral shapes were observed on the electrode surface at 100% DOD. A zoom-in of one of the spheres shows that it is composed of flakes. It is very possible that while the formation of Li_2S in the electrode makes the active particle swell, the reduction and reprecipitation of dissolved Li_2S_x formed Li_2S with an architecture of polyhedral particles by nucleating and growing at the electrode/electrolyte interface. Lin et al. also observed, through in-operando transmission X-ray microscopy, that the polysulfide redeposition is nucleation-limited that led to aggregation and dimensional variations of active particles.[44] When the cell was subsequently charged to 100%, the morphology of the electrode was similar to that of the pristine electrode. The disappearance of microsized polyhedral particles demonstrates the transformation of Li_2S back to sulfur.

Figure 3 shows the surface morphologies of a sulfur electrode after the initial discharge and subsequent charge using the

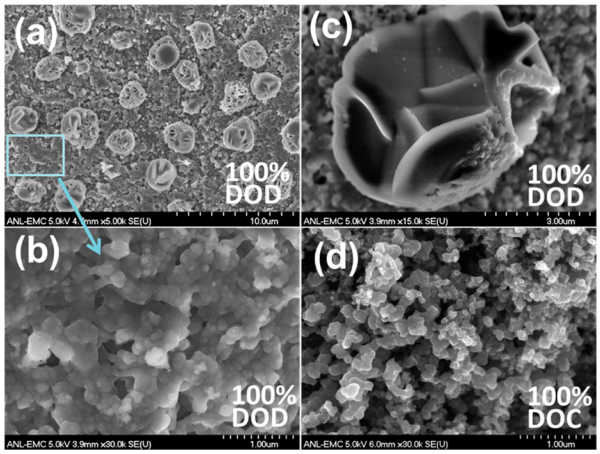

Figure 3. Surface morphology of sulfur electrode after initial discharge (a−c) and charge (d), tested using the polysulfide-based electrolyte.

Li_2S_9−$LiNO_3$ electrolyte. Similar to the cell using LiTFSI electrolyte, polyhedral particles were also formed on the surface of the completely discharged electrode, but in a larger quantity (as shown in Figure 3a,c). This finding can be explained in that the Li_2S_9−$LiNO_3$ electrolyte contains more dissolved lithium polysulfides that recrystallize into polyhedral particles during reduction. The area of the electrode surface without spheres was also much denser than that of the LiTFSI electrolyte cell. This finding suggests that the preexisting porosities in the fresh electrode were filled by discharge products. As the dissolved Li_2S_x reprecipitates at the electrode/electrolyte interface of the spheres, the Li_2S formed in the electrode was reduced from undissolved sulfur species. The denser electrode indicates the

resilience of the sulfur electrode to dissolution when the polysulfide electrolyte was present (Figure 3b). Figure 3d shows the surface morphology of the electrode with polysulfide electrolyte after the subsequent charge process. The morphology is similar to that of the pristine sulfur electrode, as shown in Figure 2.

Previously, the crystalline structure of the sulfur reduction intermediates, lithium polysulfides, had remained impervious to X-ray analysis in the laboratory because they are dissolved in organic solvents. As there is no standard X-ray diffraction pattern for Li_2S_x, we tried to probe the structure of solid lithium polysulfides. We recovered dry powders (Li_2S_4, Li_2S_6, Li_2S_8, and Li_2S_9) from lithium polysulfide solutions according to the method detailed in the Experimental Section and analyzed them by synchrotron X-ray diffraction at the Advanced Photon Source. The deposited Li_2S_x powders exhibited similar X-ray diffraction patterns, as shown in Figure 4a, which clearly demonstrates that the powders were crystalline. They contained sulfur, as indicated by the similarity of the patterns for S and Li_2S_x powders, but also a new phase or phases, as marked by asterisks. X-ray diffraction analysis on discharged sulfur electrode also shows peaks identical to those of the new phase/phases of the powders deposited from Li_2S_x solutions (as shown in Figure 4b). Cycled Li−S cells were opened at different depths of discharge, and the cathode materials were scratched from the current collector and collected for ex-situ synchrotron X-ray diffraction analysis. Figure 4b,c shows the XRD patterns of a Li−S cell using the LiTFSI- and polysulfide-based electrolytes, respectively. At 10% DOD for the electrode tested using the LiTFSI electrolyte, the sulfur peaks disappeared as all the sulfur transformed into high-order polysulfides (Li_2S_x, $x = 6–8$). At this stage it did not exhibit any X-ray diffraction peak due to the amorphous nature of the interim reduction species of sulfur. At 50% DOD, peaks appeared around 20° and 32.5° (2θ) which are identical to those noted by asterisks of the powder deposited from lithium polysulfide solution. When the discharge was completed (100% DOD), Li_2S diffraction curves appeared. The remaining minor polysulfide peaks were possibly due to the incomplete reduction to Li_2S. This result demonstrates that the sulfur was not fully utilized in the discharge in the cell using the LiTFSI electrolyte.

Although at this stage it is hard to identify the new phase in the powder deposited from the lithium polysulfide solution with a detailed structure, the results point to the possibility that this new phase is Li_2S_x. This information is helpful for further analysis and determination of the structure of the intermediate species at different electrochemical stages in Li−S batteries.

For the electrode with the polysulfide electrolyte, Figure 4c shows no polysulfide peak during the discharge, possibly because the produced polysulfides in this electrochemical environment did not crystallize. However, broader diffraction peaks of Li_2S were detected at the end of discharge, showing that the crystallization of Li_2S in the cell was not similar to that in the previous cell with the LiTFSI electrolyte. It should be noted that it is very difficult to isolate the polysulfide species in an in situ X-ray experiment, as the electrochemical sulfur system is very dynamic in the presence of dissolved polysulfides and electrolyte.

To obtain a real-time observation of the morphological and structural evolution of sulfur under real battery conditions, we performed an in situ TEM experiment in the absence of liquid electrolyte. In the experiment, a special TEM sample holder

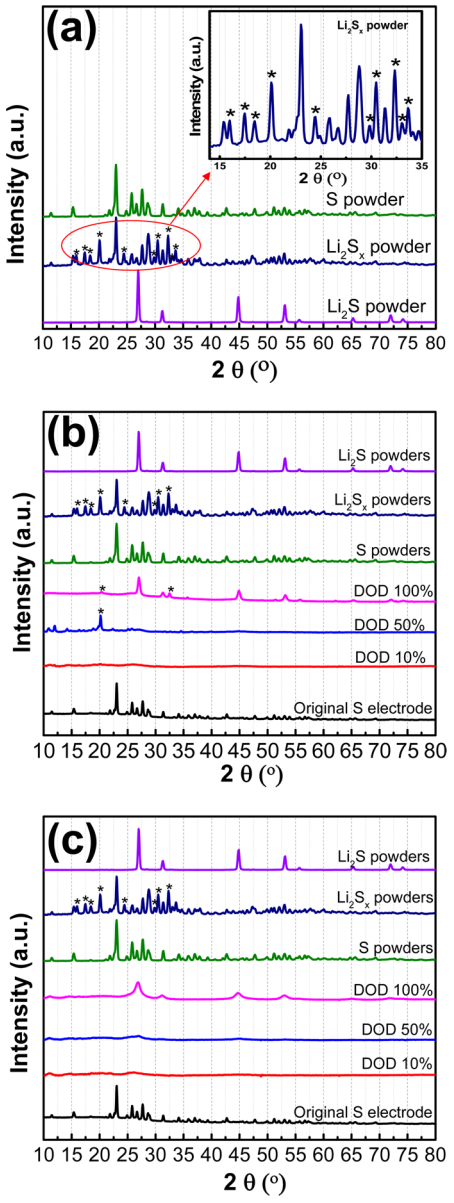

Figure 4. (a) XRD patterns of sulfur, as-prepared lithium polysulfide, and lithium sulfide. Ex situ XRD patterns of the electrode material scratched from the sulfur electrode at different depths of discharge: (b) with the LiTFSI electrolyte and (c) with the polysulfide electrolyte.

was designed to precisely control the position of a single sulfur particle and a lithium needle anode. The tip of the lithium needle was oxidized to form a thin layer of lithium oxide, which functions as a solid-state electrolyte film. A small sulfur particle was placed in the TEM sample holder in contact with the Li/Li_2O needle (as shown in Figure 5a). A negative 3 V was applied to the cell for discharge, and the system was held under a diffusion-controlled discharge process.

The discharge of the Li−S microcell took place rapidly. As observed in Figure 5b, lithium reacted with sulfur at the interface as soon as the anode was connected with sulfur, as indicated by the contrast change at the sulfur surface. After 10 s, a thin layer with a lighter contrast formed on the sulfur surface in contact with the Li/Li_2O anode. The change of the sulfur surface was recorded every 10 seconds, and the new layer spread over the outmost surface of sulfur without getting deep into the bulk of the sulfur particle.

dx.doi.org/10.1021/am504763p | ACS Appl. Mater. Interfaces 2014, 6, 21938−21945

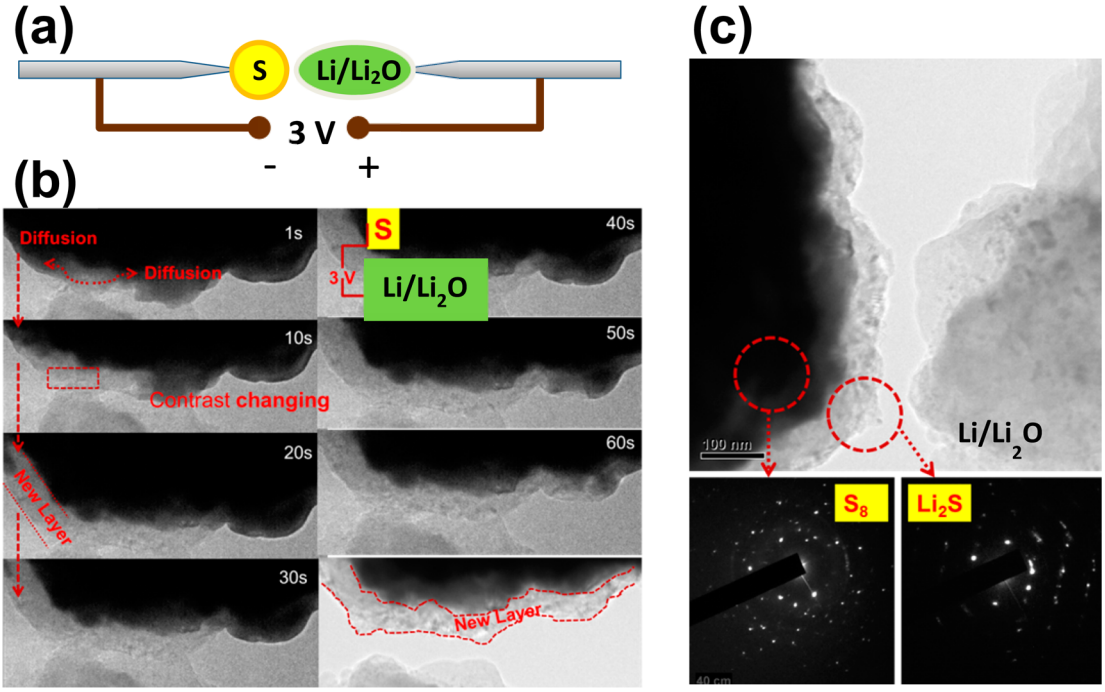

Figure 5. (a) Schematic of the Li−S cell setup for in situ TEM study, (b) TEM images of the Li−S cell during discharge (1−60 s), (c) SAED patterns of the sulfur area and the new layer.

Selected area electron diffraction (SAED) patterns of the sulfur area suggest that the new layer formed was cubic Li_2S (as shown in Figure 5c). We cannot confirm whether lithium polysulfides formed prior to Li_2S, or whether sulfur reduced directly to Li_2S in this cell. However, considering the Li−S_8 chemistry, it is more likely to be the former situation, similar to that in a cell with a liquid electrolyte. The result demonstrates that lithium diffusion preferentially occurred at the surface of the sulfur particle and formed a solid Li_2S crust on the bulk. The Li−S reaction demonstrated in Figure 5b also shows that the Li−S reaction in the cell is through surface diffusion. The insulating character of the formed Li_2S layer makes the radial diffusion of Li^+-ions through the interface into the bulk more difficult compared to that along the contour of the particle. This is in accordance with the EIS results shown in Supporting Information Figures S1−S4, which illustrate that the formation of Li_2S led to a large increase of resistance in the medium to low frequency range in the cell. While in cells with liquid electrolyte the formation and dissolution of the sulfur reduction intermediates (Li_2S_x) favor fast kinetics toward the reaction of bulk S with Li, the surface layer of Li_2S which also acts as a surface barrier must have slowed down the reaction of S with Li. This may lead to incomplete sulfur reduction during discharge in some cells, especially under comparatively high current density. For example, XRD analyses show sulfur was not fully reduced in the sulfur/acetylene black electrode with the LiTFSI electrolyte. The result suggests that because of the surface-diffusion characteristic of Li−S reaction, the use of nanoscale sulfur particles with a high specific surface area may help improve the sulfur utilization during discharge. The method of encapsulating sulfur into porous carbon as adopted in many studies breaks down the sulfur particle size and increases the sulfur surface areas, and thus usually resulted in high capacities.[9−18]

4. CONCLUSION

In summary, the performance of a Li−S cell is greatly influenced by the complex chemistry of the sulfur species, and can be significantly improved by controlling the chemical equilibria of the lithium polysulfide species in the sulfur cells. When leveling the concentration gradient of the polysulfide species at the cathode/electrolyte interface by using a polysulfide-based electrolyte, the electrode of a simple mixture of sulfur and acetylene black powders demonstrated a very stable cyclic capacity. Understanding and controlling the reduced sulfur species are essential in approaching the full theoretical capacity of Li−S cells. Therefore, various ex situ and in situ characterization methods were employed to probe the mechanism of the Li−S redox reactions and the properties of Li_2S_x and Li_2S. It was found that the dissolved Li_2S_x in the electrolyte produced Li_2S crystallites in the form of polyhedral particles at the electrolyte/electrode interface, suggesting that the reduction of these lithium polysulfides was through homogeneous nucleation. Dry powder deposited from lithium polysulfide solution was found to have a crystalline structure, as suggested by synchrotron X-ray diffraction patterns. Identical peaks were also found in discharged sulfur electrode. The results point to the possibility that the new phase in the powder deposits was Li_2S_x crystallites, although its detailed structure could not be identified at this stage. The XRD results also showed that the sulfur electrode using the LiTFSI electrolyte was not fully reduced, in agreement with the lower obtained capacity. An in situ TEM analysis during the discharge process of a Li−S cell demonstrates that lithium diffusion preferentially occurred at the surface of the sulfur particle and formed a solid Li_2S crust on the bulk. The insulating character of the formed Li_2S layer makes the radial diffusion of Li^+-ions through the interface into the bulk more difficult compared to that along the contour of the particle.

■ ASSOCIATED CONTENT

Supporting Information

Electrochemical impedance spectra (EIS) of Li−S half cells (Figures S1−S4 and list S1). Ionic conductivity test of the used electrolytes. This material is available free of charge via the Internet at http://pubs.acs.org/

■ AUTHOR INFORMATION

Corresponding Author

*E-mail: ibelharouak@qf.org.qa, belharouak@anl.gov.

Notes

The authors declare no competing financial interest.

■ ACKNOWLEDGMENTS

This research was funded by the U.S. Department of Energy, Freedom CAR, and Vehicle Technologies Office. The electron microscopy was accomplished at the Electron Microscopy Center for Materials Research at Argonne National Laboratory, a U.S. Department of Energy Office of Science Laboratory operated under Contract No. DE-AC02-06CH11357 by UChicago Argonne, LLC. The authors are also grateful to Dr. Deborah J. Mayer and Dr. Dennis W. Dees at Argonne for help in analyzing the EIS data.

■ REFERENCES

(1) Hassoun, J.; Scrosati, B. Moving to a Solid-State Configuration: A Valid Approach to Making Lithium-Sulfur Batteries Viable for Practical Applications. *Adv. Mater.* **2010**, *22*, 5198−5201.

(2) Akridge, J. R.; Mikhaylik, Y. V.; White, N. Li/S Fundamental Chemistry and Application to High-Performance Rechargeable Batteries. *Solid State Ionics* **2004**, *175*, 243−245.

(3) Ji, X.; Nazar, L. F. Advances in Li-S Batteries. *J. Mater. Chem.* **2010**, *20*, 9821−9826.

(4) Mikhaylik, Y. V.; Akridge, J. R. Low Temperature Performance of Li/S Batteries. *J. Electrochem. Soc.* **2003**, *150*, A306−A311.

(5) Xu, R.; Belharouak, I.; Zhang, X. F.; Polzin, B.; Li, J. C. M. New Developments in Lithium Sulfur Batteries *Proc. SPIE* **2013**, *8728*.

(6) Whittingham, M. S. Lithium Batteries and Cathode Materials. *Chem. Rev.* **2004**, *104*, 4271−4301.

(7) Sun, Y. K.; Myung, S. T.; Park, B. C.; Prakash, J.; Belharouak, I.; Amine, K. High-Energy Cathode Material for Long-Life and Safe Lithium Batteries. *Nat. Mater.* **2009**, *8*, 320−324.

(8) Bruce, P. G.; Freunberger, S. A.; Hardwick, L. J.; Tarascon, J. M. Li-O2 and Li-S Batteries with High Energy Storage. *Nat. Mater.* **2012**, *11*, 19−29.

(9) Ji, X.; Lee, K. T.; Nazar, L. F. A Highly Ordered Nanostructured Carbon−Sulphur Cathode for Lithium−Sulphur Batteries. *Nat. Mater.* **2009**, *8*, 500−506.

(10) Schuster, J.; He, G.; Mandlmeier, B.; Yim, T.; Lee, K. T.; Bein, T.; Nazar, L. F. Spherical Ordered Mesoporous Carbon Nanoparticles with High Porosity for Lithium-Sulfur Batteries. *Angew. Chem., Int. Ed.* **2012**, *51*, 3591−3595.

(11) Jayaprakash, N.; Shen, J.; Moganty, S. S.; Corona, A.; Archer, L. Porous Hollow Carbon@Sulfur Composites for High-Power Lithium-Sulfur Batteries. *Angew. Chem., Int. Ed.* **2011**, *50*, 5904−5908.

(12) Zheng, G. Y.; Yang, Y.; Cha, J. J.; Hong, S. S.; Cui, Y. Hollow Carbon Nanofiber-Encapsulated Sulfur Cathodes for High Specific Capacity Rechargeable Lithium Batteries. *Nano Lett.* **2011**, *11*, 4462−4467.

(13) Guo, J.; Xu, Y.; Wang, C. Sulfur-Impregnated Disordered Carbon Nanotubes Cathode for Lithium-Sulfur Batteries. *Nano Lett.* **2011**, *11*, 4288−4294.

(14) Elazari, R.; Salitra, G.; Garsuch, A.; Panchenko, A.; Aurbach, D. Sulfur-Impregnated Activated Carbon Fiber Cloth as a Binder-Free Cathode for Rechargeable Li-S Batteries. *Adv. Mater.* **2011**, *23*, 5641−5644.

(15) Zhang, B.; Qin, X.; Li, G. R.; Gao, X. P. Enhancement of Long Stability of Sulfur Cathode by Encapsulating Sulfur into Micropores of Carbon Spheres. *Energy Environ. Sci.* **2010**, *3*, 1531−1537.

(16) Wang, J. L.; Yang, J.; Xie, J. Y.; Xu, N. X.; Li, Y. Sulfur-Carbon Nano-Composite as Cathode for Rechargeable Lithium Battery Based on Gel Electrolyte. *Electrochem. Commun.* **2002**, *4*, 499−502.

(17) Sohn, H.; Gordin, M. L.; Xu, T.; Chen, S.; Lv, D.; Song, J.; Wang, D. Porous Spherical Carbon/Sulfur Nanocomposites by Aerosol-Assisted Synthesis: The Effect of Pore Structure and Morphology on Their Electrochemical Performance As Lithium/Sulfur Battery Cathodes. *ACS Appl. Mater. Interfaces* **2014**, *6*, 7596−7606.

(18) Kim, J.; Lee, D. J.; Jung, H. G.; Sun, Y. K.; Hassoun, J.; Scrosati, B. An Advanced Lithium-Sulfur Battery. *Adv. Funct. Mater.* **2013**, *23*, 1076−1080.

(19) Wu, F.; Chen, J.; Chen, R.; Wu, S.; Li, L.; Chen, S.; Zhao, T. Sulfur/Polythiophene with a Core/Shell Structure: Synthesis and Electrochemical Properties of the Cathode for Rechargeable Lithium Batteries. *J. Phys. Chem. C* **2011**, *115*, 6057−6063.

(20) Yang, Y.; Yu, G.; Cha, J. J.; Wu, H.; Vosgueritchian, M.; Yao, Y.; Bao, Z.; Cui, Y. Improving the Performance of Lithium−Sulfur Batteries by Conductive Polymer Coating. *ACS Nano* **2011**, *5*, 9187−9193.

(21) Hassoun, J.; Scrosati, B. A High-Performance Polymer Tin Sulfur Lithium Ion Battery. *Angew. Chem., Int. Ed.* **2010**, *49*, 2371−2374.

(22) He, G.; Ji, X.; Nazar, L. High "C" Rate Li-S Cathodes: Sulfur Imbibed Bimodal Porous Carbons. *Energy Environ. Sci.* **2011**, *4*, 2878−2883.

(23) Trofimov, B. A.; Myachina, G. F.; Rodionova, I. V.; Mal'kina, A. G.; Dorofeev, I. A.; Vakul'skaya, T. I.; Sinegovskaya, L. M.; Skotheim, T. A. Ethynedithiol-Based Polyeneoligosulfides as Active Cathode Materials for Lithium-Sulfur Batteries. *J. Appl. Polym. Sci.* **2008**, *107*, 784−787.

(24) Song, M. S.; Han, S. C.; Kim, H. S.; Kim, J. H.; Kim, K. T.; Kang, Y. M.; Ahn, H. J.; Dou, S. X.; Lee, J. Y. Effects of Nanosized Adsorbing Material on Electrochemical Properties of Sulfur Cathodes for Li/S Secondary Batteries. *J. Electrochem. Soc.* **2004**, *151*, A791−A795.

(25) Choi, Y. J.; Jung, B. S.; Lee, D. J.; Jeong, J. H.; Kim, K. W.; Ahn, H. J.; Cho, K. K.; Gu, H. B. Electrochemical Properties of Sulfur Electrode Containing Nano Al2O3 for Lithium/Sulfur Cell. *Phys. Scr.* **2007**, *T129*, 62−65.

(26) Ji, L.; Rao, M.; Zheng, H.; Zhang, L.; Li, Y.; Duan, W.; Guo, J.; Cairns, E. J.; Zhang, Y. Graphene Oxide as a Sulfur Immobilizer in High Performance Lithium/Sulfur Cells. *J. Am. Chem. Soc.* **2011**, *133*, 18522−18525.

(27) Kolosnitsyn, V. S.; Karaseva, E. V.; Ivanov, A. L. Electrochemistry of a Lithium Electrode in Lithium Polysulfide Solutions. *Russ. J. Electrochem.* **2008**, *44*, 564−569.

(28) Nelson, J.; Misra, S.; Yang, Y.; Jackson, A.; Liu, Y.; Wang, H.; Dai, H.; Andrews, J. C.; Cui, Y.; Toney, M. F. In operando X-ray Diffraction and Transmission X-ray Microscopy of Lithium Sulfur Batteries. *J. Am. Chem. Soc.* **2012**, *134*, 6337−6343.

(29) Liang, X.; Wen, Z.; Liu, Y.; Wu, M.; Jin, J.; Zhang, H.; Wu, X. Improved Cycling Performances of Lithium Sulfur Batteries with LiNO3-Modified Electrolyte. *J. Power Sources* **2011**, *196*, 9839−9843.

(30) Zhang, S. S.; Read, J. A. A New Direction for the Performance Improvement of Rechargeable Lithium/Sulfur Batteries. *J. Power Sources* **2012**, *200*, 77−82.

(31) Aurbach, D.; Pollak, E.; Elazari, R.; Salitra, G.; Kelley, C. S.; Affinito, J. On the Surface Chemical Aspects of Very High Energy Density, Rechargeable Li-Sulfur Batteries. *J. Electrochem. Soc.* **2009**, *156*, A694−A702.

(32) Trofimov, B. A.; Markova, M. V.; Morozova, L. V.; Prozorova, G. F.; Korzhova, S. A.; Cho, V. D.; Annenkov, V. V.; Mikhaleva, A. I. Protected Bis(hydroxyorganyl) Polysulfides as Modifiers of Li/S Battery Electrolyte. *Electrochim. Acta* **2011**, *56*, 2458−2463.

(33) Xu, R.; Belharouak, I.; Li, J. C. M.; Zhang, X.; Bloom, I.; Bareño, J. Role of Polysulfides in Self-Healing Lithium-Sulfur Batteries. *Adv. Energy Mater.* **2013**, *3*, 833−838.
(34) Xu, R.; Zhang, X.; Yu, C.; Ren, Y.; Li, J. C. M.; Belharouak, I. Paving the Way for Using Li2S Batteries. *ChemSusChem* **2014**, *7*, 2457−2460.
(35) Cheon, S. E.; Ko, K. S.; Cho, J. H.; Kim, S. W.; Chin, E. Y.; Kim, H. T. Rechargeable Lithium Sulfur Battery I. Structural Change of Sulfur Cathode During Discharge and Charge. *J. Electrochem. Soc.* **2003**, *150*, A796−A799.
(36) Canas, N. A.; Wolf, S.; Wagner, N.; Friedrich, K. A. In-Situ X-ray Diffraction Studies of Lithium−Sulfur Batteries. *J. Power Sources* **2013**, *226*, 313−319.
(37) Barchasz, C.; Molton, F.; Duboc, C.; Lepretre, J. C.; Patoux, S.; Alloin, F. Lithium/Sulfur Cell Discharge Mechanism: An Original Approach for Intermediate Species Identification. *Anal. Chem.* **2012**, *84*, 3973−3980.
(38) Mikhaylik, Y. V.; Akridge, J. R. Polysulfide Shuttle Study in the Li/S Battery System. *J. Electrochem. Soc.* **2004**, *151*, A1969−A1976.
(39) Diao, Y.; Xie, K.; Xiong, S. Z.; Hong, X. B. Analysis of Polysulfide Dissolved in Electrolyte in Discharge-Charge Process of Li-S Battery. *J. Electrochem. Soc.* **2012**, *159*, A421−A425.
(40) Canas, N. A.; Hirose, K.; Pascucci, B.; Wagner, N.; Friedrich, K. A.; Hiesgen, R. Investigations of Lithium−Sulfur Batteries Using Electrochemical Impedance Spectroscopy. *Electrochim. Acta* **2013**, *97*, 42−51.
(41) Kolosnitsyn, V. S.; Kuzmina, E. V.; Karaseva, E. V.; Mochalov, S. E. A Study of the Electrochemical Processes in Lithium−Sulphur Cells by Impedance Spectroscopy. *J. Power Sources* **2011**, *196*, 1478−1482.
(42) Cuisinier, M.; Cabelguen, P. E.; Evers, S.; He, G.; Kolbeck, M.; Garsuch, A.; Bolin, T.; Balasubramanian, M.; Nazar, L. F. Sulfur Speciation in Li−S Batteries Determined by Operando X-ray Absorption Spectroscopy. *J. Phys. Chem. Lett.* **2013**, *4*, 3227−3232.
(43) Kawase, A.; Shirai, S.; Yamoto, Y.; Arakawa, R.; Takata, T. Electrochemical Reactions of Lithium−Sulfur Batteries: An Analytical Study Using the Organic Conversion Technique. *Phys. Chem. Chem. Phys.* **2014**, *16*, 9344−9350.
(44) Lin, C. N.; Chen, W. C.; Song, Y. F.; Wang, C. C.; Tsai, L. D.; Wu, N. L. Understanding Dynamics of Polysulfide Dissolution and Re-deposition in Working Lithium−Sulfur Battery by in-Operando Transmission X-ray Microscopy. *J. Power Sources* **2014**, *263*, 98−103.
(45) Lowe, M. A.; Gao, J.; Abruña, H. D. Mechanistic Insights into Operational Lithium−Sulfur Batteries by in Situ X-ray Diffraction and Absorption Spectroscopy. *RSC Adv.* **2014**, *4*, 18347−18353.
(46) Lu, Y. C.; He, Q.; Gasteiger, H. A. Probing the Lithium−Sulfur Redox Reactions: A Rotating-Ring Disk Electrode Study. *J. Phys. Chem. C* **2014**, *118*, 5733−5741.